Amphiphilic Dendritic Molecules: Hyperbranched Polyesters with Alkyl-Terminated Branches

X. Zhai,[†] S. Peleshanko,[†] N. S. Klimenko,[‡] K. L. Genson,[†] D. Vaknin,[§] M. Ya. Vortman,[‡] V. V. Shevchenko,[‡] and V. V. Tsukruk*,[†]

Department of Materials Science and Engineering, Iowa State University, Ames, Iowa 50011; Institute of Macromolecular Chemistry, Kiev, 02160, Ukraine; and Ames Laboratory and Department of Physics and Astronomy, Iowa State University, Ames, Iowa 50011

Received August 26, 2002

ABSTRACT: We report on the synthesis of a series of second-generation hyperbranched polyesters with a variable composition of alkyl-terminated groups. We observed that the chemical modification of the hyperbranched cores by substituting a controlled fraction of the terminal hydroxyl groups with hydrophobic alkyl chains is an effective method for a controlling amphiphilic balance of hyperbranched cores with a degree of branching of 50%. Even for imperfect cores, the chemical reaction of hydroxyl groups alkyl tails was very efficient. In fact, the number of attached alkyl tails was fairly close to the theoretical value based on the assumption that all targeted hydroxyl groups were available for the reaction despite their different interior/exterior location. Detailed microstructural analysis of the structure revealed that organized monolayers could be formed at the air−water interface if the number of alkyl tails was higher than two per core. Similar to regular dendrimers, the alkyl tails of hyperbranched molecules at high surface pressure form intramonolayer ordering of the quasi-hexagonal type. However, higher defectness and irregularities of the hyperbranched cores are responsible for poor intralayer ordering of alkyl tails in comparison with regular dendrimers. At high surface pressure, the alkyl tails became arranged in an up-right orientation. The highly water-swollen state of the hyperbranched cores of prolate shape and the partially submerged and standing-off alkyl tails is a characteristic of hyperbranched molecules with fewer alkyl chains in condensed monolayer state at the air−water interface. The core structure is transformed into the oblate, flattened state with preservation of standing-off orientation of the alkyl tails for hyperbranched molecules with crowded outer shells.

Introduction

Dendritic polymers have attracted significant interest due to their promising properties of combined functionalized macromolecules and nanoparticles.[1−3] Hyperbranched polymers and dendrimers represent two major and different classes of such materials. Contrary to highly regular dendrimers obtained in a multistep processes, hyperbranched polymers are synthesized in one pot. The morphology and overall shape of dendritic molecules and their interfacial behavior can be controlled through the internal chemical architecture, the nature and distribution of terminal groups, and the strength of the molecule−surface interactions.[4−9] Despite significant polydispersity and inherit defectness of their chemical structure caused by internal cyclization and side reactions, hyperbranched polymers possess, to a great extent, all major elements, which are characteristics of compact nanoparticle-like structures with significant fraction of terminal groups located on the exterior of the molecules.[10−14] However, in contrast to the highly regular dendrimers, the hyperbranched polymers did not show sharp transitions and exhibited a macroscopic spreading behavior similar to that of isotropic liquids.[15]

Discrete molecules and their surface aggregates were observed while studying adsorption of hyperbranched molecules formed from a four-functional core and AB_2 monomer.[16] Molecular dimensions were consistent with theoretical estimates and molecules sustained significant external stresses. To design dendritic molecules capable of forming organized aggregates and monolayers at interfaces, amphiphilic balance should be introduced by appropriate modification of terminal groups with e.g., hydrophobic tails. Several examples of such a modification focused on balance of hydrophobic and hydrophilic interactions have been reported for both regular dendrimers and hyperbranched polymers.[6,17] The fabrication of stable Langmuir monolayers at the air−water interfaces and Langmuir−Blodgett (LB) monolayers on a solid substrate have been reported for dendrimers with polar cores and hydrophobic shells. Conformational flexibility of dendrimer branches allowed for the folding of the dendritic structure and forming a pancake shape of the polar cores at the air−water interface. Stable monolayers were formed with the alkyl chains aligned perpendicular to the water surface and the dendritic core in a pancake conformation facing the aqueous phase.[18] This model suggested that significant flexibility of the dendritic cores provides for conformational reorganization, resulting in an overall shape compatible with the planar air−water interface. Only higher generation dendrimers showed surface irregularities of the monolayers, which were attributed to space constraints imposed by the shell−core branched structure.[19,20] Hyperbranched polyesters with epoxy-containing alkyl tails were used for the fabrication of robust elastic monolayers with residual surface functionality.[21]

Much less attention has been devoted to structural studies of the series of the hyperbranched polymers with

[†] Department of Materials Science and Engineering, Iowa State University.
[‡] Institute of Macromolecular Chemistry.
[§] Ames Laboratory and Department of Physics and Astronomy, Iowa State University.
* To whom correspondence should be addressed: e-mail vladimir@iastate.edu.

10.1021/ma021383j CCC: $25.00 © 2003 American Chemical Society
Published on Web 03/18/2003

systematically modified terminal groups. Adding long-chain terminal alkyl groups has been reported by Johansson et al. for hydroxyl-terminated hyperbranched polyesters.[22] Three generations of hyperbranched polymers based on 2,2-bis(hydroxymethyl)propionic acid (bis-MPA) and 3,3,7,7-tetra(hydroxymethyl)-5-oxanonan (di-TMP) as a core were modified with dodecanoyl alkyl tails. Rheological behavior of that modified hyperbranched polymers was controlled by the number of alkyl groups rather than overall size of hyperbranched molecules. Moore et al. demonstrated a strong influence of terminal group modification on the surface properties of the hyperbranched polymers.[6] These data for hyperbranched polymers were consistent with a high effectiveness of the end functionalities for regular dendrimers.[6,18,23] However, it is still not clear how the inherently imperfect chemical microstructure of the hyperbranched cores affects overall composition of the functionalized hyperbranched molecules and their ability to conformational transformations required to adapt hydrophilic−hydrophobic layered structure at the air−water interfaces. Screening of some interior functional groups could affect the efficiency of their chemical modification and, thus, the core−shell balance. Irregular branched structure, internal cyclization, uneven functionality of branches, interior vs exterior location of terminal groups, and the polydispersity of the molecules all could affect the efficiency of the modification of functional terminal groups and their resulting interfacial properties.

In this study, we report on the synthesis of a series of hyperbranched polyesters (**HP-*N***) with a systematically changing number of the terminal alkyl groups attached to the polar core of a second generation. We focus on analyzing the chemical composition of these alkyl-modified hyperbranched molecules and studying their interfacial behavior and internal microstructure at the air−water interface and at a solid surface. Conditions for the fabrication of stable Langmuir monolayers are identified, and peculiarities of internal microstructure related to the presence of the hyperbranched cores are revealed.

Experimental Section

Materials. Tetrahydrofuran (THF, HPLC grade), chloroform (Reagent grade), and methyl alcohol (Reagent grade) were purchased from Fisher Scientific Co. and used as received. 2-Ethyl-2-hydroxymethyl-1,3-propanediol (TMP, Aldrich, 99%) was dried by heating under vacuum. Stearoyl chloride was synthesized by a reaction of stearic acid with PCl_5 and distilled before use, and dimethylformamide (DMF) was carefully dried. 2,2-Bis(hydroxymethyl)propionic acid (bis-MPA), *p*-toluenesulfonic acid (*p*-TSA), triethylamine (TEA), and hexane (95+%) were used as received from Aldrich.

Characterization. ^{13}C and ^{1}H NMR spectra were recorded on a Varian VXR-400 MHz using DMSO-d_6 according to a method described by Malström et al.[22,24] Fourier transform infrared (FTIR) measurements were conducted on a Schimadzu 8300 spectrometer in attenuated total reflection (ATR) mode. Gel permeation chromatography (GPC) measurements were carried out to monitor trends in the variation of molecular weight as measured against polystyrene standards. These measurements were conducted in THF solution using a Waters Breeze 1500 system. Differential scanning calorimetry (DSC) studies were conducted on a Pyris 1 instrument (Perkin-Elmer).

The surface behavior of hyperbranched molecules was studied at the air−water interface, and LB monolayer deposition was conducted using a LB trough (R&K 1, Germany). 15 μL of dilute HPs solution in chloroform was deposited onto the Nanopure ($\Omega \geq 18.0$ MOm cm) water surface of the LB trough. The concentration of a **HP** solution in chloroform was in the range 0.5−1 mmol/L. Barriers on either side of the trough applied equal loads and compressed at the rate of 50 μm/s. The monolayers were deposited onto silicon substrates at low and high surface pressures, 15 and 35 mN/m.

The thickness of the deposited layer was measured with a Compel ellipsometer (InOmTech, Inc.). The average thickness of the SiO_2 layer was measured prior to the layer deposition and used during analysis of the ellipsometry data with a double-layer model.[25] The refractive indices were taken from literature data for polyesters and estimated from molar contribution for hyperbranched polymers.[26,27] The monolayers on a silicon surface were studied with an atomic force microscope (AFM) Dimension 3000 (Digital Instrument, Inc.) in the tapping mode according to an experimental procedure described earlier.[28] The imaging was performed in the regime of the "light" tapping to avoid damaging of the monolayers.

X-ray grazing incident diffraction (XGID) and X-ray reflectivity measurements from Langmuir monolayers at the air−water interface were conducted on a liquid-surface X-ray spectrometer at the 6ID beam line at the Advanced Photon Source synchrotron at Argonne National Laboratory according to the usual procedure described elsewhere.[29−31] Details regarding X-ray reflectivity and XGID and the experimental setup are described elsewhere.[32] During the synchrotron experiments, the LB trough was placed in a helium environment to reduce the background scattering and prevent an oxidation reaction that can damage the monolayer.

The box model was used to determine the electron densities across the interface and to relate them to the molecular arrangements of the molecular fragments at the interface.[33] The box model consists of slabs of differing thickness and electronic density stacked above the water subphase with known electron density (330 e/nm^3). The interfaces are smeared to account for the surface roughness and thermal vibrations. The arrangement of the molecular segments can be determined from the length and electron density of the boxes via direct comparison with molecular models. The simulated reflectivity used to fit the experimental data was calculated from

$$R(Q_z) = R_0(Q_z)\mathrm{e}^{-(Q_z\sigma)^2} \quad (1)$$

where the $R_0(Q_z)$ is the reflectivity from steplike functions and σ is the surface roughness. The reflectivity calculated for various trial electronic density profiles was compared with experimental results during the fitting procedure.

Molecular modeling was performed on a SGI workstation with the Cerius^2 3.9 program.[34] The data were primary used for the visualization of the molecular shape and the estimation of the most probable molecular dimensions. For the model with separate packing of a polar core and alkyl tails, the core in a flattened conformation was used, and the alkyl branches were added in a predominantly vertical position before dynamic mechanics and energy minimization were executed.

Synthesis of Hyperbranched Polymers. All synthetic procedures were made under a dry nitrogen atmosphere. Hyperbranched polyester−polyol of a second generation with TMP as a core and bis-MPA was prepared by a procedure described in the literature (Figure 1).[22] Esterification was carried out at 140 °C with *p*-TSA as an acid catalyst. The chosen TMP:bis-MPA molar ratio 1:9 corresponded to the theoretical molecular weight of 1179 g/mol and a hyperbranched polymer with 12 terminal hydroxyl groups. The crude polymer was precipitated from acetone in hexane and dried under vacuum. FTIR showed no remaining carboxylic acid.

$C_{17}H_{35}$ alkyl tails were attached by the reaction of terminal hydroxyl groups with stearoyl chloride in DMF in the presence of TEA as an acceptor of HCl. As the reaction proceeds, TEA hydrochloride precipitates from the reaction medium, and its quantity corresponds to consumed stearoyl chloride. The number of consumed stearoyl chloride corresponded to 10, 25, 50, and 75% hydroxyl groups in **HP-0** (+10% excess). Corresponding specimens are designated as **HP-10**, **HP-25**, **HP-50**, and **HP-75**. All compounds were low-melting materials

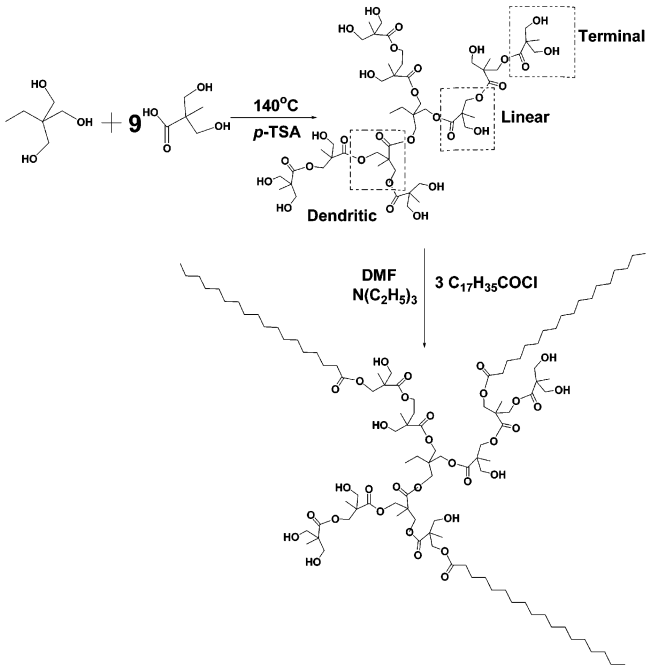

Figure 1. Reaction scheme for **HP-0** and chemical formulas for **HP-0** and **HP-25** molecules.

Table 1. Characteristics of Compounds HP-*N*

compd	M_n theoretical	M_n (g/mol)	M_w (g/mol)	M_w/M_n
HP-0	1179	979	1350	1.38
HP-10	1498	1154	1795	1.55
HP-25	1977	1046	1626	1.55
HP-50	2775	1975	2494	1.26
HP-75	3573	2160	2973	1.38

soluble in most organic solvents. As the number of alkyl chains in polymer increased, HB compounds became insoluble in water. For example, for **HP-25**, we used a 50 mL three-neck flask equipped with a magnetic stirrer, a dry nitrogen inlet, and a drying tube. Compound **HP-0** (4.0 g, 3.39 mmol) and triethylamine (1.13 g, 11.2 mmol) were dissolved in DMF (25 mL). A freshly prepared solution of stearoyl chloride (3.39 g, 11.2 mmol) in DMF (5 mL) was added slowly and dropwise. The mixture was kept under stirring at room temperature for 1 h. A precipitate of triethylamine hydrochloride was filtered off, and the solvent was removed under vacuum. A residue was washed several times with cold hexane. In the same way, compounds **HP-10**, **HP-25**, **HP-50**, and **HP-75** were synthesized. Attempts to obtain 100% substituted molecules were not successful. The molecular characteristics of all compounds are given in Table 1.

The hyperbranched core had a ^{1}H NMR spectrum with the following parameters: δ 1.04 (s, $-CH_3$), 1.09 (s $-CH_3$), 1.18 (s, $-CH_3$), 3.47 (q, $-CH_2-OH$), 4.03−4.12 (m, $-CH_2$), 4.62 (br s, −OH), 4.93 (br s, −OH). The values obtained were close to those reported by Malstrom et al.[22,24] For alkyl-modified compounds, we observed an appearance of the new bands associated with alkyl tails: δ 0.83 (t, $-CH_3$), 1.15−1.28 (m, $-CH_3$, $-CH_2$, 1.5 (t, $-CH_2CH_2COO-$), 2.3 (t, $-CH_2CH_2COO-$).

Results and Discussion

Chemical Composition. Idealized chemical structures of hyperbranched polymers based on the polyester−polyol core with hydroxyl-terminated groups (**HP-0**) and 25% substitution of the hydroxyl terminal groups by alkyl tails, $C_{17}H_{35}$, **HP-25**, are presented in Figure 1. The number of hydroxyl groups (12) in the idealized second-generation core **HP-0** was evaluated from the initial composition of chemical compounds involved in the reaction. The molecular characteristics of synthesized compounds are shown in Table 1.

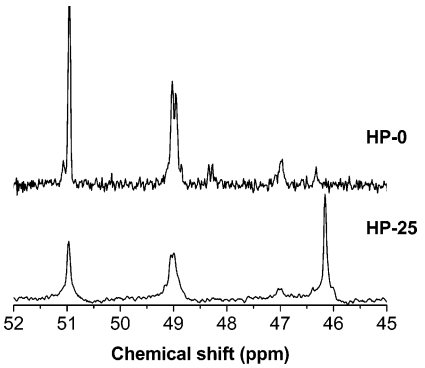

Figure 2. ^{13}C NMR spectra of compounds **HP-0** and **HP-25**.

NMR data confirmed the chemical composition and the branching structure of compounds (Figure 2). Each repeating unit within the hyperbranched core was associated with the following chemical shift difference on ^{13}C NMR spectra: T, terminal unit (ppm), 50.65, L, linear unit (ppm), 48.85, D, dendritic unit (ppm), 46.80 of the quaternary carbon (Figure 2).[22,23] The degree of branching (DB) for hyperbranched polymers based on AB_2 monomers is defined according to Hawker et al.[5] as follows:

$$DB = (\Sigma D + \Sigma T)/(\Sigma D + \Sigma T + \Sigma L) \qquad (2)$$

where ΣD, ΣT, and ΣL are total contributions from dendritic, terminal, and linear units, respectively (Figure 1).

According to ^{13}C NMR data, the initial core retained a similar degree of branching for compounds studied varying from 46% to 52%. This is close to the theoretical estimation and indicates the presence of a significant fraction of linear fragments. At this level of branching, estimated eight hydroxyl groups should be present on the exterior of the molecule, and four groups should be located in the interior space of the molecule as indicated by a model in Figure 1. Strong overlapping of several peaks on the NMR spectra prevented unambiguous evaluation of a number of alkyl tails in the alkyl-modified molecules. GPC data showed molecular weight distribution with a polydispersity index of 1.3−1.6 that indicates modest polydispersity of the hyperbranched molecules similar to previously reported values (Table 1).[22,35]

FTIR spectra for **HP-0** confirmed the targeted chemical microstructure. Spectra for the initial core were similar to ones reported previously for a similar hyperbranched core and (Figure 3).[35] They showed no adsorption bands related to the remaining carboxylic acid but only ester bands (1730 cm^{-1}, C═O) that indicated completeness of the substitution reactions (Figure 3).[36] A strong and broad peak around 3200−3600 cm^{-1} and a small peak at 530 cm^{-1} confirmed a high concentration of hydroxyl groups in the **HP-0** molecule.[36] An increase of content of $C_{17}H_{35}$ branches resulted in systematic reduction of the intensity of these adsorption bands and a rising intensity of a double peak at 2920 and 2880 cm^{-1},which corresponds to a CH_2 stretching vibration (Figure 3). The variation of the peak intensity of CH_2 and OH groups vs a degree of substitution presented shows a gradual increase of the alkyl tail content and corresponding decrease of the amount of the terminal hydroxyl groups (Figure 4a). However, these data can-

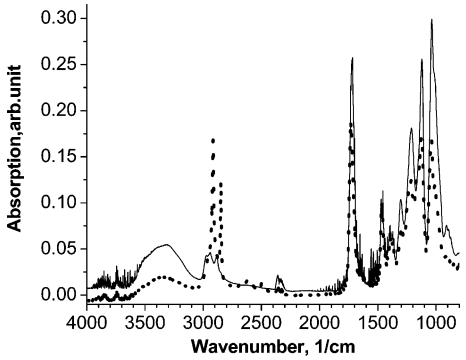

Figure 3. FTIR spectra for **HP-0** (solid) and **HP-75** (dot) compounds.

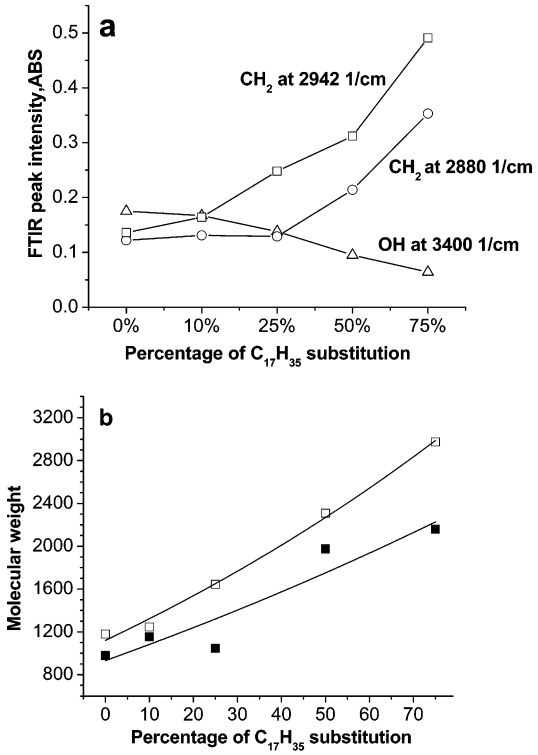

Figure 4. (a) Variation of intensities of CH_2 and OH bands of FTIR spectra with composition. (b) Theoretical (squares) and GPC-measured (filled squares) molecular weights as a function of degree of substitution.

not provide measures of internal chemical composition in quantitative terms.

The molecular weight of the alkyl-terminated hyperbranched compounds showed a virtually linear increase with substitution content (Figure 4b). The experimentally measured molecular weights were systematically lower than the theoretical values obtained from the idealized models that indicate less perfect chemical microstructure (Table 1). However, because PS standard-based GPC measurements underestimate the molecular weight of dendritic macromolecules, a discussion of significance of these differences on a quantitative level is meaningful.[35,37]

DSC studies of modified hyperbranched materials revealed the presence of melting points in the temperature range 40−60 °C and glass transition temperatures below −30 °C (not shown). These transitions are clearly related to melting of alkyl tails and the glass transition of hyperbranched cores, respectively.[38] These separate transitions indicate highly phase-separated microstructure with independent packing and crystallization of terminal alkyl branches and hyperbranched cores similar to modified regular dendrimers.[39]

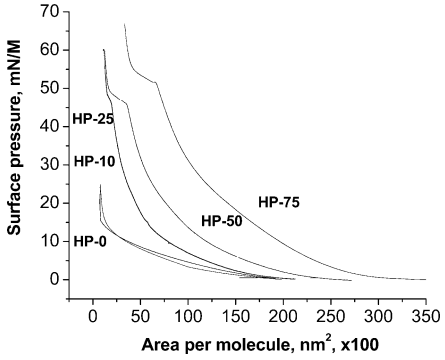

Figure 5. Pressure−area isotherms for Langmuir monolayers fabricated from compounds **HP-0**, **HP-10**, **HP-25**, **HP-50**, and **HP-75**. The molecular weight of the molecules was taken from GPC data.

Behavior at the Air−Water Interface. The surface compression behavior of hyperbranched polymers depends strongly upon the actual number of hydrophobic tails attached to the polar core. The reproducible and reversible $\pi-A$ isotherms were obtained for the hyperbranched compounds with higher than 25% of branches terminated with alkyl tails (Figure 5). Both the core itself and the alkyl-modified compound with low content of alkyl tails, **HP-10**, were gradually dissolving in the subphase during compression. The reproducible isotherms for the hyperbranched compounds with 25−75% substitution showed a steady increase in the surface pressure upon compression that is indicative of the formation of stable Langmuir monolayers with liquid and solid 2D phase formation typical for the amphiphilic compounds.[40]

The surface area per molecule, A_0, was calculated by the extrapolation of the steep rise in the surface pressure to a zero level in accordance with a usual procedure.[41] Numerical values can be obtained from such an extrapolation only if the molecular weight of the molecules is a known parameter. Because of the unknown structure of the molecules, no direct comparison between valid molecular models and the actual data can be made without certain assumptions. First, we used a molecular weight from an idealized molecular composition as a limiting case (overestimated molecular weight, column 1 in Table 1). Second, a molecular weight from GPC data was used as a representative of another limiting case (underestimated molecular weight, column 2 in Table 1). The actual unknown molecular weight is somewhere between these two limits. The comparison of the idealized structure of the hyperbranched core and molecular area of the core given by the limiting area of the LB isotherm is limited in this study because we have no direct measurement of the area of the core, theoretical or experimental. Therefore, the discussion of the results will be mainly limited to the degree of substitution of the alkyl tails.

The surface area per molecules calculated from the surface area isotherms under these two assumptions is presented in Figure 6. Both sets of data show remarkable linear increase with increasing substitution content and differ from each other by an overall slope of this relationship. The difference in the surface areas per molecule for the highest content of alkyl substitution calculated under two different assumptions does not

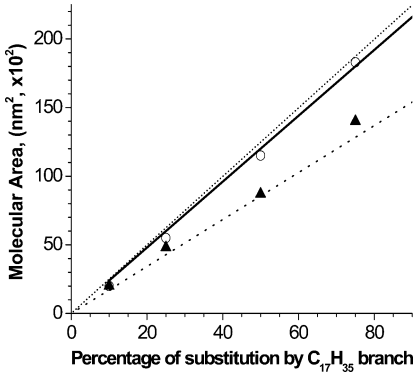

Figure 6. Variation of the surface area per molecule estimated from different models: experimentally observed molecular area from the pressure−area isotherms (solid); molecular area estimated for the molecules with molecular weight taken from the theoretical model (○); molecular area estimated for the molecules with molecular weight taken from GPC data (▲).

exceed 30−40%. Thus, taking the known surface area per alkyl tail in a solid monolayer state as 0.2 nm^2, we can estimate a number of alkyl tails per molecule participating in the formation of the monolayers (Table 2).[41] We observed that the values obtained under the "ideal" assumption were close to the "theoretical" number of alkyl tails per molecule, and another limiting case gave 1−2 less tails per molecule. Considering that two possible limiting cases have been included in our estimations, we can conclude that the LB data confirms a high degree of substitution with not more that 1−2 alkyl tails missing for the substitution of 50% and higher.

Table 2. Estimated Number of Terminal Alkyl Tails

	idealized number[a]	estimated from LB isotherm (MW from GPC)	estimated from LB isotherm (MW from model)
HP-0	0	0	0
HP-10	1.2	1	1
HP-25	3	2.4	2.8
HP-50	6	4.4	5.8
HP-75	9	7	9.1

[a] Calculated for chemical formula presented in Figure 1.

Hence, for the formation of stable monolayer structures, at least two C_{17} alkyl tails should be attached to the polar core. This suggest that at least 30% of the total mass of the molecule should be hydrophobic to prevent "sinking" of the water-soluble polar cores in the water subphase. Our finding on the surface behavior is similar to that reported for regular alkyl-terminated dendrimers.[17,18] The cross-sectional area occupied by alkyl tails is close to minimal possible area for the chains in upright position. This points out that the compression of the Langmuir monolayers should result in similar internal reorganization of the alkyl-terminated dendritic structure as proposed for regular flexible dendrimers with regular core structure.[18]

A key feature of this model is the formation of hydrophilic and hydrophobic layers composed of different molecular segments in the condensed monolayers (Figure 7). A first layer, bordering with the water subphase, is composed of a polar core. A second, outer layer is formed by standing-off alkyl tails. Although it is impossible to estimate the volume of polar core quantitatively due to the unknown water content and packing density (X-ray data discussed below give only

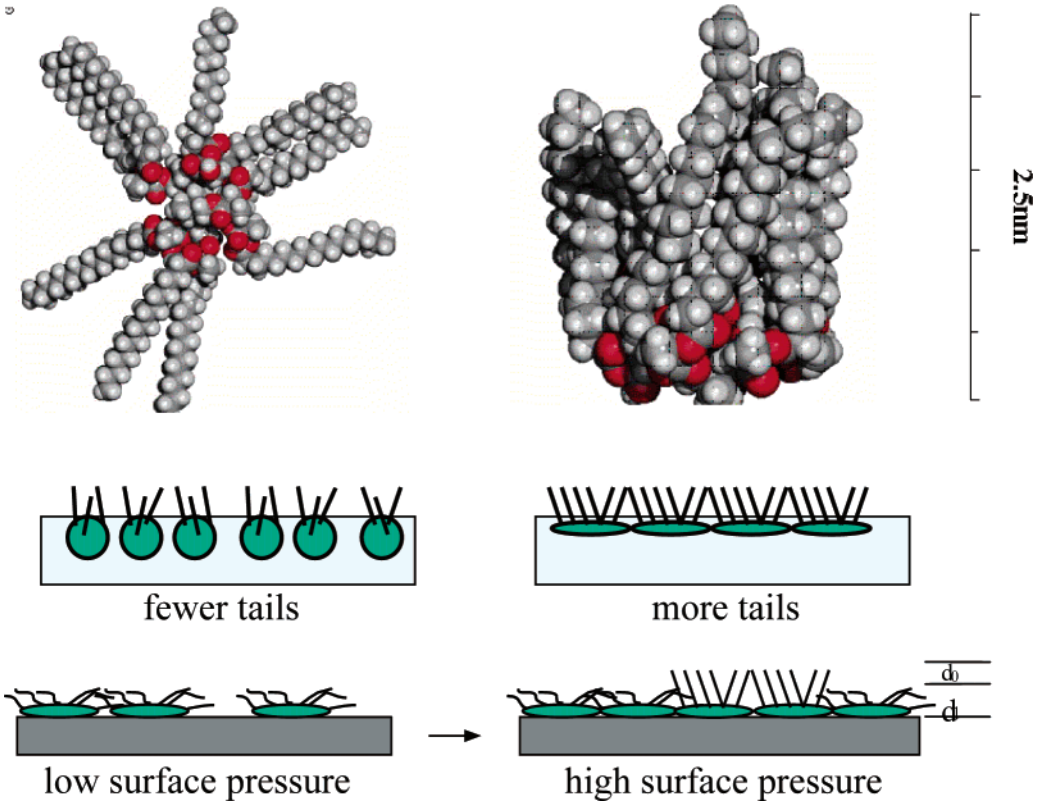

Figure 7. Top: models of a modified hyperbranched polymer with a random orientation of alkyl terminal tails (left) and in a compressed state with a standing-off orientation of alkyl tails and flattened polar core (right). Center: sketches of molecular conformation in condensed monolayer state for molecules with low (left) and high (right) number of alkyl tails. Bottom: sketches of molecular packing for Langmuir monolayer at low (left) and high (right) surface pressures with thickness presented in Table 5.

estimates), some conclusions can be made on molecular shape from general considerations of molecular volume and molecular areas. From molecular dimensions, the molar volume of polar core could be estimated to be larger than 1 nm^3. Thus, for molecules with two−three alkyl chains (**HP-25**) compressed to molecular area of 0.5 nm^2, the only choice for the polar core could be the formation of cylindrical or prolate shape with a diameter of 0.8 nm. Assuming the same water content, the height of such a cylindrical core structure could be estimated as close to 2 nm. For the **HP-50** molecule, a more crowded shell results in increasing cross-sectional area per molecule to 0.9 nm^2, and thus the height of the core structure should be close to 1.1 nm. Finally, for the highest number of the terminal alkyl tails attached, the molecular area of 1.3−1.5 nm^2 should result in an oblate, squashed shape of the hyperbranched core with a thickness of 0.6−0.8 nm (Figure 7). Apparently, to ensure up-right position of the alkyl tails, the hyperbranched core should adapt a flattened conformation different from one with a random orientation of branches and terminal groups (Figure 7). Although this model seems to be a natural choice that explains our surface isotherm results, additional evidence from X-ray reflectivity and grazing angle diffraction and AFM investigations need to confirm this picture (see below).

In fact, in recent studies, Kampf et al. found evidence that the molecular weight increase associated with the increase in generation number caused monodendrons that initially form a vertically elongated shape on the water surface to flatten.[42] Conformational flexibility of regular dendrimers cores was proven to be sufficient for this compression. Large steric constraints were observed to be responsible for flattening of dendrimers cores in higher generation dendrimers. On the other hand, significant role of submerging capability of polar cores on ordering of hydrophobic shells was demonstrated for monodendrons.[20,43] Similarly, we see the increase in the number of attached alkyl tails forces the hydrophilic core to flatten on the surface and submerge in the subphase to allow the hydrophobic tails to organize at the surface. As has been recently shown, a hyperbranched molecule based on a dendritic polyester core can expand in favorable solvent conditions to nearly twice its original size, demonstrating significant conformational flexibility of hyperbranched cores, which can facilitate structural changes discussed here.[44] Percec et al. showed that by increasing the degree of functionalization at the periphery the solid angle of the molecule is increased.[45] By controlling the solid angle of the molecular shape, the size of the molecule can be controlled and the packing structure tailored to the desired outcome. Here we see the increase of alkyl tails attached to the hyperbranched core increases the favorability of the core flattening on the water surface, allowing the alkyl tails to organize better into lateral packing structures.

Molecular Ordering of Langmuir Monolayers. All GIXD studies of Langmuir monolayers at surface pressures below ∼15 mN/m have no detectable diffraction peaks incidating no lateral ordering of alkyl tails at the lower surface pressures. A single broad peak in intermediate wave-vector range that corresponds to a solid-state phase shows up for all three samples at higher surface pressure (Figure 8). The single peak for **HP-25** is positioned at $Q_{xy} = 15.1$ nm^{-1} corresponding

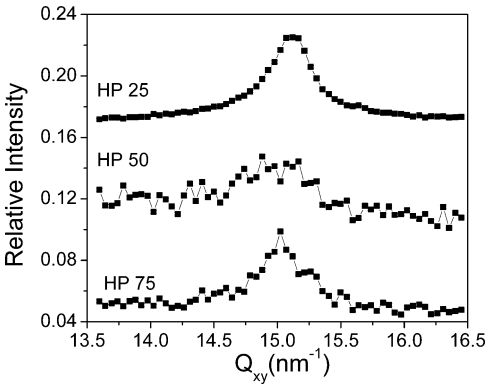

Figure 8. Comparison of the observed X-ray diffraction data of the monolayer of the hyperbranched compounds at the highest surface pressure. The original intensities are offset for clarity.

Table 3. Structural Parameters of Intralayer Packing for Langmuir Monolayers Obtained from X-ray Diffraction

	HP-25	HP-50	HP-75
d-spacing (nm)	0.416	0.419	0.419
unit cell parameter, *a* (nm)	0.480	0.484	0.484
correlation length (nm)	4.63	3.19	6.15

to a 0.416 nm *d* spacing, and its position remains virtually unchanged for other hyperbranched molecules (Table 3). The appearance of a single peak centered near $Q_{xy} = 15.0$ nm^{-1} suggests a hexagonal lateral packing of alkyl tails with six equivalent neighboring tails. The calculated hexagonal unit cell parameter for all monolayers is within the range 0.480−0.484 nm, which is typical for alkyl tails that are normal to the water surface.[42,43] This confirms conclusions made from LB experiments. Additionally, out-of-plane rod scans at the Bragg peaks (not shown) confirm upright orientation of alkyl tails.

The diffuse nature of the diffraction peaks suggests limited ordering of the alkyl tails of liquid-crystalline type within the monolayers.[46,47] The limited intralayer ordering of the alkyl tails with monolayers is characteristic of the outer shell of amphiphilic dendritic molecules. Reduced ordering and suppression of crystallization are caused by space constraints imposed by the chemical attachment of tails to highly branched structures as suggested in recent studies.[48] Calculated intralayer correlation lengths are much smaller than that for "free" alkyl chain in linear amphiphilic molecules and for alkyl tails from outer shells of regular dendrimers and monodendrons (30−100 nm[20,43,48,49]) and vary from 3.2 to 6.2 nm (Table 3). We suggest that this difference can be associated with much defect internal structure of hyperbranched cores as compared to regular branched structure of dendrimers. Irregular branching and random attachments of the terminal alkyl tails prevent the formation of regular intralayer ordering and crystallization of alkyl tails usually observed for dendrimers molecules. The highest correlation length for molecules with the highest number of alkyl tails (**HP-75**) suggests that high density of grafting of the alkyl tails to the hyperbranched core is critical for the formation of more ordered lateral packing less disturbed by the flattened polar core.

The X-ray reflectivity data and corresponding fits for lower and higher surface pressures for all compounds are shown in Figure 9. The best fit for the **HP-25** compound at both surface pressures can be obtained

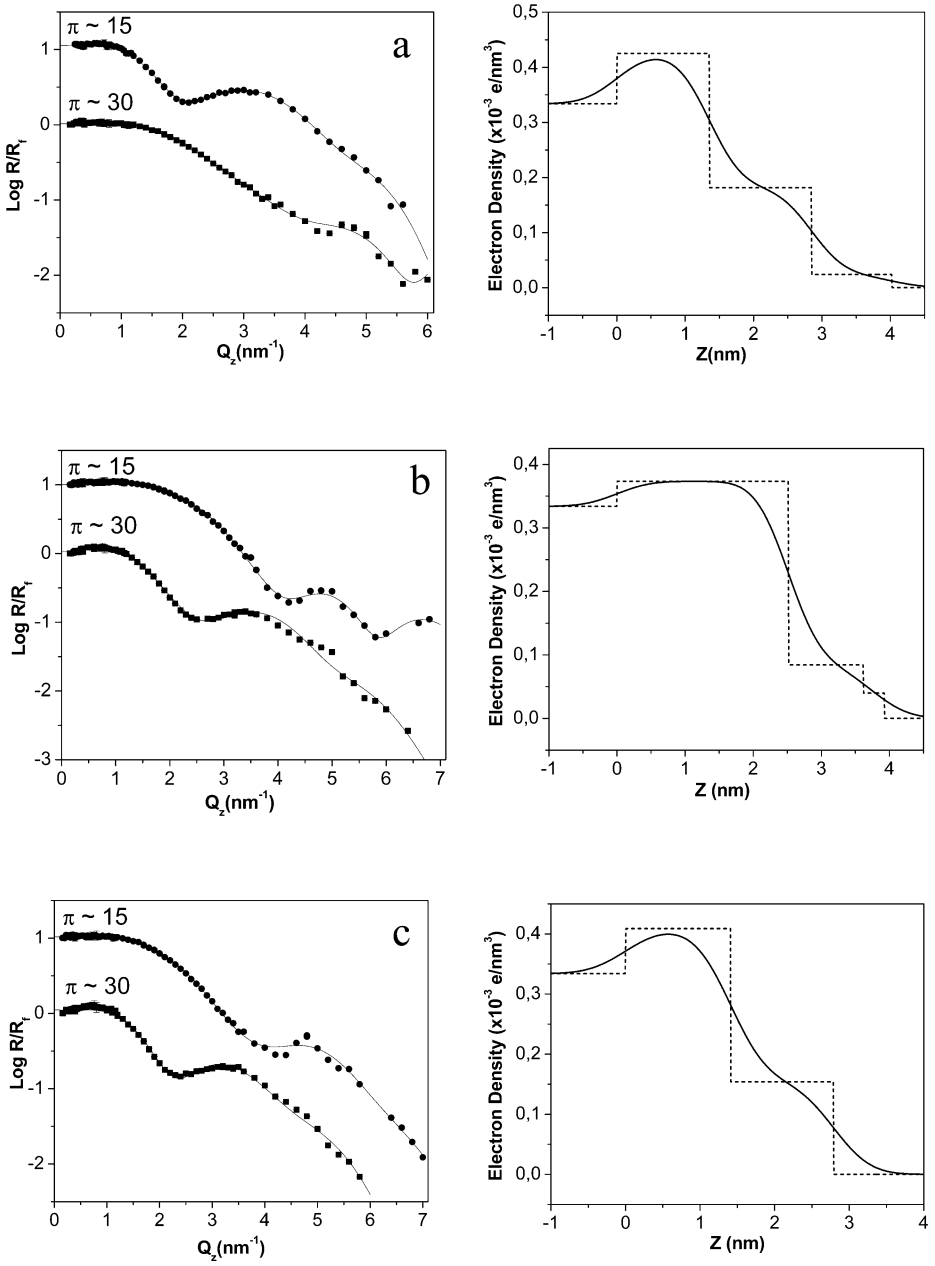

Figure 9. X-ray reflectivity data at the air−water interface for (a) **HP-25**, (b) **HP-50**, and (c) **HP-75** with the best fits. The symbols represent the experimental data while the solid lines represent the best fits. For the corresponding box models, dashed lines represent initial box models and solid lines show smeared profiles with surface roughness.

Table 4. Electron Density Distribution Parameters along the Surface Normal Obtained from the Reflectivity Data for Three Compounds at Both Surface Pressures

	HP-25		HP-50		HP-75	
pressure (mN/m)	15	30	15	30	15	30
first box length (nm)	1.52	1.36	1.47	2.52	1.54	1.41
first box density ($\times 10^{-3}$ e/nm^3)	0.38	0.42	0.42	0.37	0.40	0.41
second box length (nm)	0.615	1.49	0.61	1.10	0.56	1.38
second box density ($\times 10^{-3}$ e/nm^3)	0.18	0.18	0.18	0.084	0.15	0.15
third box length (nm)	0.91	1.18	0.97	0.31	0.72	
third box density ($\times 10^{-3}$ e/nm^3)	0.047	0.024	0.064	0.04	0.066	
fourth box length (nm)			1.07		1.39	
fourth box density ($\times 10^{-3}$ e/nm^3)			0.019		0.014	
roughness[a] (nm)	0.24	0.39	0.31	0.39	0.34	0.39
total length of tails (nm)	1.53	2.67	2.65	1.41	2.67	1.38

[a] Roughness is for all transitions between the elements of the fitting model.

using a three-box model with a box with higher electron density for the hyperbranched core and shorter boxes with lower electron density stacked on top to represent the alkyl tails (Figure 9, Table 4). The low electron density of the third box suggest the tails do not order in a uniform layer but create a staggered layer with a limited number of tails reaching the third box and/or lateral domain microstructure. The third box in the

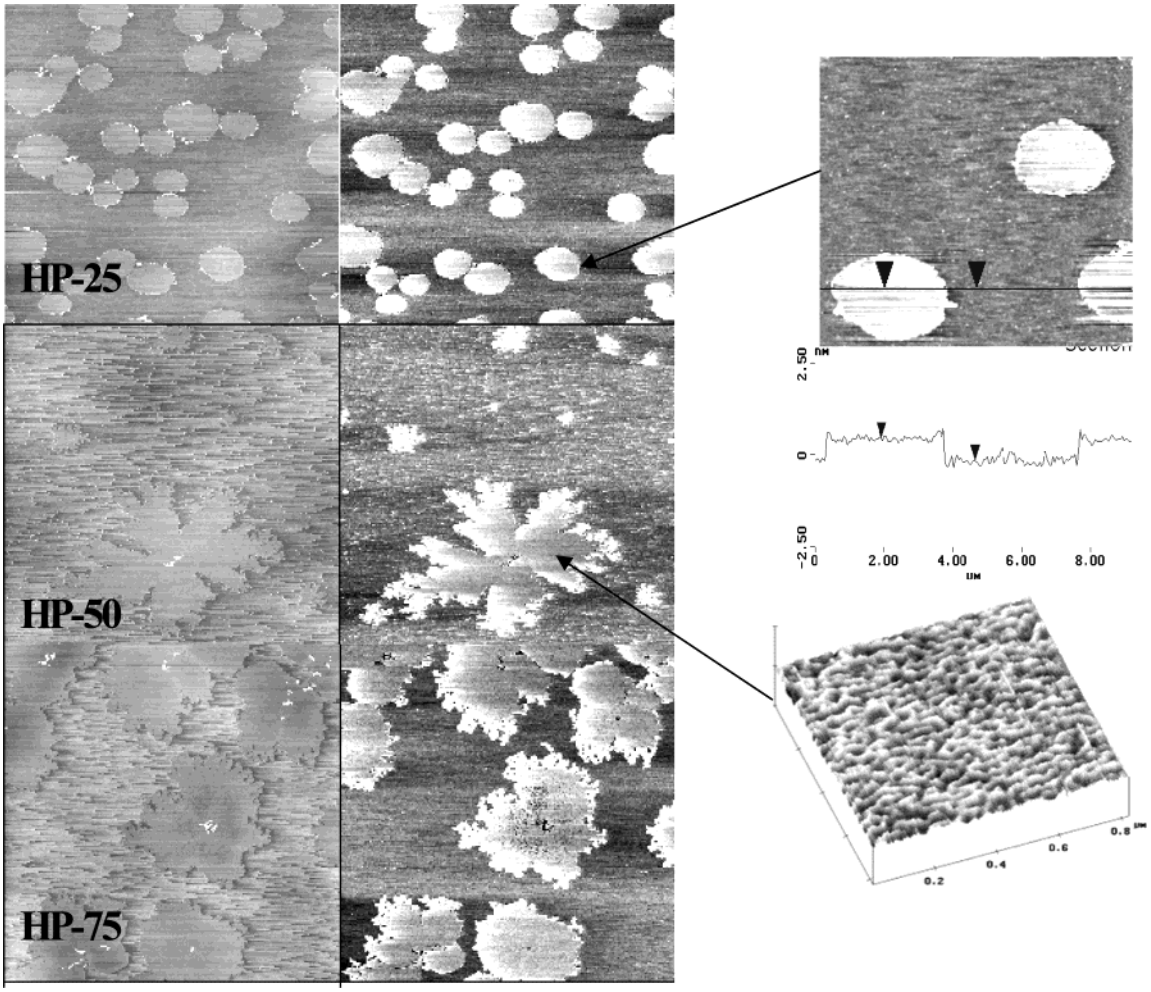

Figure 10. AFM images of LB monolayers for all amphiphilic hyperbranched compounds studied deposited at the surface pressure of 35 mN/m (topography (left) and phase (right)). Scan size is 25 × 25 μm, height scale is 20 nm, and phase scale is 30°. Zoom-in image (8 × 8 μm) and the corresponding cross section of the domain structures for **HP-25** (top, right) and surface morphology of domains at high resolution (800 × 800 nm) (bottom, right).

models is most likely from a higher surface roughness than expected.

The lower surface pressure monolayers **HP-50** and **HP-75** are best fit with a four-box model with a higher electron density box representing the core and three lower electron density boxes representing the interlayer with alkyl tails. The lower densities of the top two boxes again reveal a staggered nature in the packing structure of the tails, suggesting a limited number of tails reach the upper most boxes and/or a small fraction of the surface area is covered with domains with a thickness higher than the average thickness of the monolayer. The total thickness of the alkyl tail interlayer is close to the length of the tails in standing-off orientation for molecules with 25% of conversion (Table 4). For molecules with a higher content of grafted tails (50% and 75%), the thickness of this interlayer is smaller, which suggests inclusion of part of the alkyl tails tethered to the branches in the interlayer formed by the water-soluble hyperbranched cores (Figure 7).

The higher surface pressure data for **HP-50** can be fit using a three-box model with the third box of extremely low electron density similar to the model for higher surface pressure **HP-25**. The best fit for the **HP-75** higher surface pressure data is a two-box model with two boxes of similar length but significantly different electron density. The first box is assigned to the hyperbranched core, and the second is assigned to the alkyl tails. However, for some compounds this box could include both submerged cores and partially submerged tails. The density of the second box suggests that the alkyl tails are not densely packed due to the developed domain microstructure. Comparison of the calculated number of electrons from the box models to the number of electrons expected from the molecular models indicates that the hyperbranched cores are, indeed, submerged in the water subphase and contain 50−80 water molecules. Therefore, X-ray studies of the Langmuir monolayers confirm the model with standing-off alkyl tails proposed from the pressure−area isotherms and suggests specific quantitative characteristics of this type of ordering summarized in Tables 3 and 4 and Figure 7.

Microstructure of Monolayers on a Solid Surface. AFM imaging confirms domain microstructure of the monolayers under the surface pressure studied. Figure 10 shows selected AFM images of the LB monolayers deposited on a bare silicon substrate at the surface pressure of 35 mN/m. Aggregate domain microstructure associated with usual two-phase state (solid−liquid) of the monolayers could be clearly observed. The diameter of these domains changed with the degree of $C_{17}H_{35}$ substitution. The shape of the domains for **HP-25** was approximately round, and they had a uniform

Table 5. Thickness of LB Monolayers on Solid Substrate As Obtained from AFM and Ellipsomtery

	theoretical height,[a] nm	thickness by ellipsometry, nm		thickness by AFM, nm (monolayers deposited at 35 mN/m)		
		15 mN/m	35 mN/m	domain height d_0	height of matrix d_1	total thickness
HP-25	2.0	1.13	1.73	0.6	1.25	1. 85
HP-50	2.5	1.31	2.04	0.8	1.52	2.32
HP-75	2.5	1.33	2.09	0.8	1.54	2.34

[a] Calculated from molecular models with uniformly vertically oriented tails.

diameter, in the range from 2 to 4 μm. Domains were flat with fine internal structure visible within these domains at high magnification and microroughness within 1 × 1 μm area below 1 nm (Figure 10). For the hyperbranched polymers with a higher content of alkyl tails, the domain became larger (6−10 μm in diameter) with a dendritic shape composed of several anisotropic domains growing from a single center.

The height of domains, obtained from AFM cross-section analysis, was within 0.6−0.8 nm as calculated from the reference level of the surrounding monolayer surface (Figure 10, Table 5). Considering these morphologies and X-ray reflectivity data, we conclude that they support a biphasic model of the monolayer microstructure (Figure 7). This model suggests that a "matrix" monolayer in a "liquid" state is formed by the hyperbranched cores and alkyl tails in random conformation similar to a low-pressure monolayer. The height of deposited monolayers outside of domain areas of 1.25−1.62 nm was close to that of the monolayers deposited at low surface pressure (1.13−1.33 nm). This further proved that the matrix monolayers were formed by the hyperbranched molecules with predominantly randomly oriented tails.

However, a significant fraction of the monolayer deposited at higher surface pressure was occupied by thicker domains formed by molecules with alkyl tails in standing-off orientation as suggested by X-ray reflectivity analysis. Indeed, the thickness of "matrix" monolayer determined from independent AFM measurements of scratched areas was within 1.2−1.6 nm that give an effective thickness of domains about within 2.3−2.4 nm that was close to the thickness expected for the model with standing-off alkyl tails (Figure 7, Table 5). Apparently, more compact vertical packing of the monolayers deposited on a solid surface determined from AFM as compared to the same monolayers at the air−water interface determined by X-ray reflectivity (see Tables 4 and 5) was caused by removal of water from the hyperbranched cores during their deposition onto a solid substrate.

Conclusions

In conclusion, we synthesized a series of alkyl-terminated, hyperbranched polyesters with a variable amphiphilic core−shell balance. We demonstrated that the chemical modification of the hyperbranched polymers by substituting a controlled fraction of the terminal hydroxyl groups with alkyl chains is an effective method of a controlled fabrication of organized monolayers at the air−water interfaces and solid surfaces from these dendritic molecules. We found that, despite the fact that the degree of branching of imperfect polyester cores was 50%, the chemical reaction of substitution of the hydroxyl groups with the alkyl tails was very efficient. The number of alkyl tails attached to the branches was fairly close to the theoretical expectations based on assumption that all targeted hydroxyl groups were available for the reaction despite their inequivalency due to interior/exterior locations.

Detailed microstructural analysis of the interfacial ordering revealed that organized monolayers with distinct domain structure are formed at both air−water interface and solid surfaces if a number of alkyl tails is higher than two−three per the polyester core of second generation. At high surface pressure, the alkyl tails became arranged in an up-right orientation with dense liquid-crystalline ordering of the quasi-hexagonal type. The water-swollen state of the hyperbranched cores of the prolate shape and the partially submerged standing-off alkyl tails is a characteristic of the hyperbranched molecules with fewer alkyl chains in the condensed monolayer state at the air−water interface. The core structure is transformed into the oblate, flattened state with preservation of standing-off orientation of the alkyl tails for hyperbranched molecules with crowded outer shells. We suggest that irregular branching and random attachments of the terminal alkyl tails in the hyperbranched molecules prevent the formation of regular lateral ordering and crystallization of the alkyl tails within Langmuir monolayers usually observed for modified dendrimers molecules.

Acknowledgment. Funding from the National Science Foundation, DMR-0074241, and Imperial Chemical Industries (GPC instrumentation) is gratefully acknowledged. The Midwest Universities Collaborative Access Team (MUCAT) sector at the APS, where X-ray studies were conducted, is supported by the U.S. Department of Energy, Basic Energy Sciences, Office of Science, through the Ames Laboratory under Contract W-7405-Eng-82. Use of the APS was supported by the U.S. Department of Energy, Basic Energy Services, Office of Science, under Contract W-31-109-Eng-38. The authors thank M. Ornatska and M. LeMieux for technical assistance during experiments and Prof. V. P. Privalko for sharing DSC results for low temperatures.

References and Notes

(1) *Dendrimers and Other Dendritic Polymers*; Fréchet, J. M. J., Tomalia, D. A., Eds.; John Wiley & Sons: New York, 2002. Frechet, J. M. *Science* **1994**, *263*, 1711. Tomalia, D. A. *Adv. Mater.* **1994**, *6*, 529. Grayson, S. M.; Frechet, J. M. J. *Chem. Rev.* **2001**, *101*, 3819. Percec, V.; Chu, P.; Ungar, G.; Zhou, J. *J. Am. Chem. Soc.* **1995**, *117*, 11441.

(2) *Dendritic Molecules*; Newkome, G. R., Moorefield, C. N., Vogtle, F., Eds.; VCH: Weinheim, 1996. Meijer, E. W. *Science* **1994**, *266*, 1226.

(3) Frechet, J. M.; Hawker, G. J.; Gitsov, I.; Leon, J. W. *Pure Appl. Chem.* **1996**, *A33*, 1399. Sastry, M.; Gole, A.; Sainkar, S. R. *Langmuir* **2000**, *16*, 3553. Collier, C. P.; Saykally, R. J.; Shiang, J. J.; Henrichs, S. E.; Heath, J. R. *Science* **1997**, *277*, 1978. Damle, C.; Cole, S.; Sastry, M. *J. Mater. Chem.* **2000**, *10*, 1389. Sayed-Sweet, Y.; Hedstrand, D. M.; Spinder, R.; Tomalia, D. *J. Mater. Chem.* **1997**, *7*, 1199. Saville, P. M.; Reynolds, P. A.; White, J. W.; Hawker, C. J.; Frechet, J. M.; Wooley, K. L.; Penfold, J.; Webster, J. R. *J. Chem. Phys.* **1995**, *99*, 8283.

(4) Wells, M.; Crooks, R. M. *J. Am. Chem. Soc.* **1996**, *118*, 3988.

(5) Young, J. K.; Baker, G. R.; Newkome, G. R.; Morris, K. F.; Johnson, C. S. *Macromolecules* **1994**, *27*, 3464.
(6) Savill, P. A.; Reynolds, P. A.; White, J. W.; Hawker, C. J.; Frechet, J. M. J.; Wooley, K. L.; Penfold, J.; Webster, J. R. P. *J. Phys. Chem.* **1995**, *99*, 8283.
(7) Iyer, J.; Hammond, P. T. *Langmuir* **1999**, *15*, 1299.
(8) Tsukruk, V. V. *Adv. Mater.* **1998**, *10*, 253. Tsukruk, V. V.; Rinderspacher, F.; Bliznyuk, V. N. *Langmuir* **1997**, *13*, 2171. Bliznyuk, V. N.; Rinderspacher, F.; Tsukruk, V. V. *Polymer* **1998**, *39*, 5249.
(9) Tully, D. C.; Frechet, M. J. *Chem. Commun.* **2001**, 1229.
(10) Kim, Y. H.; Webster, O. W. *J. Am. Chem. Soc.* **1990**, *112*, 4592.
(11) Hawker, C. J.; Lee, R.; Frechet, J. M. J. *J. Am. Chem. Soc.* **1991**, *113*, 4583.
(12) Voit, B. *J. Polym. Sci., Part A* **2000**, *38*, 2505. Orlicki, J. A.; Thompson, J. L.; Markoski, L. J.; Sill, K. N.; Moore, J. S. *J. Polym. Sci., Polym. Chem.* **2002**, *40*, 936. Markoski, L. J.; Moore, J. S.; Sendijarevic, I.; McHugh, A. J. *Macromolecules* **2001**, *34*, 2695.
(13) Sheiko, S. S.; Gauthier, M.; Moller, M. *Macromolecules* **1997**, *30*, 2343. Sheiko, S. S.; Buzin, A. I.; Muzafarov, A. M.; Rebrov, E. A.; Getmanova, E. V. *Langmuir* **1998**, *14*, 7468.
(14) Mackay, M. E.; Carmezini, G.; Sauer, B. B.; Kampert, W. *Langmuir* **2001**, *17*, 1708.
(15) Voit, B. *J. Polym. Sci., Part A* **2000**, *38*, 2505. Hult, A.; Johansson, M.; Malmstrom, E. *Adv. Polym. Sci.* **1999**, *143*, 1. Ihre, H.; Johansson, M.; Malmstrom, E.; Hult, A. *Adv. Dendritic Macromol.* **1996**, *3*, 1. Voit, B. *J. Polym. Sci., Part A* **2000**, *38*, 2505. Mueller, A.; Kowalewski, T.; Wooley, K. L. *Macromolecules* **1998**, *31*, 776. Zhang, X.; Klein, J.; Sheiko, S.; Muzafarov, A. M. *Langmuir* **2000**, *16*, 3893. Mezzenga, R.; Boogh, L.; Manson, J.-A. E.; Pettersson, B. *Macromolecules* **2000**, *33*, 4373.
(16) Sidorenko, A.; Zhai, X. W.; Peleshanko, S.; Greco, A.; Shevchenko, V. V.; Tsukruk, V. V. *Langmuir* **2001**, *17*, 5924.
(17) Stevelmans, S.; van Hest, J. C. M.; Jansen, J. F. G. A.; van Boxtel, D. A. F. J.; de Brabander-van den Berg, E. M. M.; Meijer, E. W. *J. Am. Chem. Soc.* **1996**, *118*, 7398. Morgenroth, F.; Berresheim, A. J.; Wagner, M.; Mullen, K. *Chem. Commun.* **1998**, 1139. Ramzi, A.; Bauer, B. J.; Scherrenberg, R.; Froehling, P.; Joosten, J.; Amis, E. J. *Macromolecules* **1999**, *32*, 4983. Loi, S.; Wiesler, U. M.; Butt, H.-J.; Mullen, K. *Macromolecules* **2001**, *34*, 3661. Liebau, M.; Janssen, H. M.; Inoue, K.; Shinkai, S.; Huskens, J.; Sijbesma, R. P.; Meijer, E. W.; Reinhoudt, D. N. *Langmuir* **2002**, *18*, 674. Tsiourvas, D.; Stathopoulou, K.; Sideratou, Z.; Paleos, C. M. *Macromolecules* **2002**, *35*, 1746.
(18) Schenning, A. P. H. J.; Elissen-Roman, C.; Weener, J.-W.; Baars, M. W. P. L.; Van der Gaast, S. J.; Meijer, E. W. *J. Am. Chem. Soc.* **1998**, *120*, 8199.
(19) Johnson, M. A.; Santini, C. M.; Iyer, J.; Satija, S.; Ivkov, R.; Hammond, P. T. *Macromolecules* **2002**, *35*, 231.
(20) Genson, K. L.; Vaknin, D.; Villavicencio, O.; McGrath, D.; Tsukruk, V. V. *J. Phys. Chem.* **2002**, *106*, 11277.
(21) Sidorenko, A.; Zhai, X. W.; Tsukruk, V. V. *Langmuir* **2002**, *18*, 3408. Sidorenko, A.; Zhai, X. W.; Simon, F.; Pleul, D.; Greco, A.; Tsukruk, V. V. *Macromolecules* **2002**, *35*, 5131.
(22) Malmstrom, E.; Johansson, M.; Hult, A. *Macromolecules* **1995**, *28*, 1698. Johansson, M.; Malmstrom, E.; Hult, A. *J. Polym. Sci., Polym. Chem.* **1993**, *31*, 619.
(23) Jikei, M.; Kakimoto, M. *Prog. Polym. Sci.* **2001**, *26*, 1233.
(24) Magnusson, H.; Malstrom, E.; Hult, A. *Macromolecules* **2000**, *33*, 3099.
(25) Azzam, R. M. A.; Bashara, N. M. *Ellipsometry and Polarized Light*; North-Holland Pub. Co.: Amsterdam, 1977.
(26) Aranishi, Y.; Takahashi, H. *Jpn. Kokai Tokkyo Koho* **2000**, 6. JKXXAF JP 2000226727 A2 20000815.
(27) Van Krevelen, D. W. *Properties of Polymers*; Elsevier: Amsterdam, 1997.
(28) Tsukruk, V. V.; Reneker, D. H. *Polymer* **1995**, *36*, 1791. Tsukruk, V. V. *Rubber Chem. Technol.* **1997**, *70*, 430. *Scanning Probe Microscopy of Polymers*; Ratner, B., Tsukruk, V. V., Eds.; ACS Symposium Series; American Chemical Society: Washington, DC, 1998; p 694.
(29) Bohm, C.; Leveiller, F.; Jacquemain, D.; Mohwald, H.; Kjaer, K.; Als-Nielsen, J.; Weissbuch, I.; Leiserowitz, L. *Langmuir* **1994**, *10*, 830.
(30) Weissbuch, I.; Leveiller, F.; Jacquemain, D.; Kjaer, K.; Als-Nielsen, J.; Leiserowitz, L. *J. Phys. Chem.* **1993**, *97*, 12858.
(31) Vaknin, D.; Kelley, M. S. *Biophys. J.* **2000**, *79*, 2616.
(32) Vankin, D. In *Methods of Materials Research*; Kaufmann, E. N., Abbaschian, R., Barnes, P. A., Bocarsly, A. B., Chien, C. L., Doyle, B. L., Fultz, B., Leibowitz, L., Mason, T., Sanchez, J. M., Eds.; John Wiley & Sons: New York, 2001; p 10d.2.1.
(33) Gregory, B. W.; Vaknin, D.; Gray, J. D.; Ocko, B. M.; Stroeve, P.; Cotton, T. M.; Struve, W. S. *J. Phys. Chem. B* **1997**, *101*, 2006.
(34) Cerius^2 3.9; Molecular Simulations Inc.: San Diego, CA, 1997.
(35) Jang, J.; Oh, J. H. *Polymer* **1999**, *40*, 5985.
(36) Workman, J. *Handbook of Organic Compounds*; Academic Press: San Diego, CA, 2001.
(37) Kim, Y. H. *J. Polym. Sci., Polym. Chem.* **1998**, *36*, 1685.
(38) Low-temperature DSC data were provided by Prof. V. Privalko.
(39) Ihre, H.; Hult, A.; Frechet, A.; Gitsov, I. *Macromolecules* **1998**, *31*, 4061.
(40) Ulman, A. *Introduction to Ultrathin Organic Films*; Academic Press: San Diego, CA, 1991.
(41) Small, D. M. *The Physical Chemistry of Lipids*; Plenum Press: New York, 1986.
(42) Kampf, J. P.; Frank, C. W.; Malmstrom, E. E.; Hawker, C. J. *Langmuir* **1999**, *15*, 227.
(43) Pao, W.; Stetzer, M. R.; Heiney, P. A.; Cho, W.; Percec, V. *J. Phys. Chem. B* **2001**, *105*, 2170.
(44) Mackay, M. E.; Carmezini, G. *Chem. Mater.* **2002**, *14*, 819.
(45) Percec, V.; Cho, W.-D.; Ungar, G. *J. Am. Chem. Soc.* **2000**, *122*, 10273.
(46) Kaganer, V. M.; Mohwald, H.; Dutta, P. *Rev. Mod. Phys.* **1999**, *71*, 779.
(47) Tsukruk, V. V.; Shilov, V. V. *Structure of Liquid Crystalline Polymers*; Naukova Dumka: Kiev, 1990.
(48) Larson, K.; Vaknin, D.; Villavicencio, O.; McGrath, D.; Tsukruk, V. V. *J. Phys. Chem. B* **2002**, *106*, 7246.
(49) Kaganer, V. M.; Osipov, M. A.; Peterson, I. R. *J. Chem. Phys.* **1993**, *98*, 3512.

MA021383J